Chapter 44
Experimental Studies of the Matrix Detonating Cord Charge

Vilem Petr and Steven Beggs

Abstract The objective of the study is to validate and advance the understanding of the Matrix detonating cord charge. This paper examines the functionality of the Matrix charge and compares the propagation and shock wave behavior to sheet explosive charges (deta-sheet). This was achieved through a series of tests in which the charges were detonated underwater in an aquarium and observed with ultra high speed imaging instrumentation. The team successfully recorded and documented various detonation events involving simple and complex charge geometries. The data enabled the team to measure velocity of detonation (VOD) values, analyze shock front propagation and analyze shockwave interaction. Tests results show that the sheet explosive produces a symmetrical and uniform incident shock wave, and the Matrix charge produces multiple incident shock waves, which collide and reflect, and generate Mach stem waves.

Keywords Detonating cord • Sheet explosive • Mach stem • Detonation physics • High-speed imaging

44.1 Introduction

Public Safety bomb technicians and ATF agents routinely dispose of unstable explosive materials and homemade explosives mixtures using a high explosive counter charge known as the Matrix charge. The ATF National Center for Explosives Training and Research (NCETR) designed the Matrix charge to improve the safety and effectiveness of explosive disposal operations.

The Matrix charge is field constructed from a single length of detonating cord woven into a grid to form a "net" of detonating cord (Fig. 44.1). The Matrix charge may be constructed using any strength of detonating cord (grains per foot) and can be configured to any size or area specification. The charge is constructed using the Matrix Field Assembly Tool (Fig. 44.2). The tool and charge were granted a U.S. Patent (Patent# US 7,913,624 B2) in 2011 and are now extensively used in the United States by public safety bomb technicians.

The objective of this study is to examine the functionality of the Matrix charge and compare its propagation and shock wave behavior to sheet explosives. The team designed a series of sixteen (16) tests in which various charges were detonated underwater in an aquarium and observed with ultra high-speed imaging instrumentation.

44.2 Experimental Setup and Procedures

The tests were conducted at the AXPRO Small Scale Explosive Laboratory (Fig. 44.3) at Colorado School of Mines (CSM) campus. A Specialized Imaging SIMX 16 ultra high-speed digital camera equipped with 80–200 mm Tokina lens (F-stop: 4.5; zoom: 80; focus: 3.1 m) was the primary instrumentation used in the tests. Figure 44.4 depicts the test set-up and instrumentation arrangement.

V. Petr (✉)
Technical Director AXPRO Group, Colorado School of Mines, 1500 Illinois Street, Golden, CO 80401, USA
e-mail: vpetr@mines.edu

S. Beggs
Research Associate A-T Solutions, Inc., Golden, CO, USA

B. Song et al. (eds.), *Dynamic Behavior of Materials, Volume 1: Proceedings of the 2014 Annual Conference on Experimental and Applied Mechanics*, Conference Proceedings of the Society for Experimental Mechanics Series,
DOI 10.1007/978-3-319-06995-1_44,

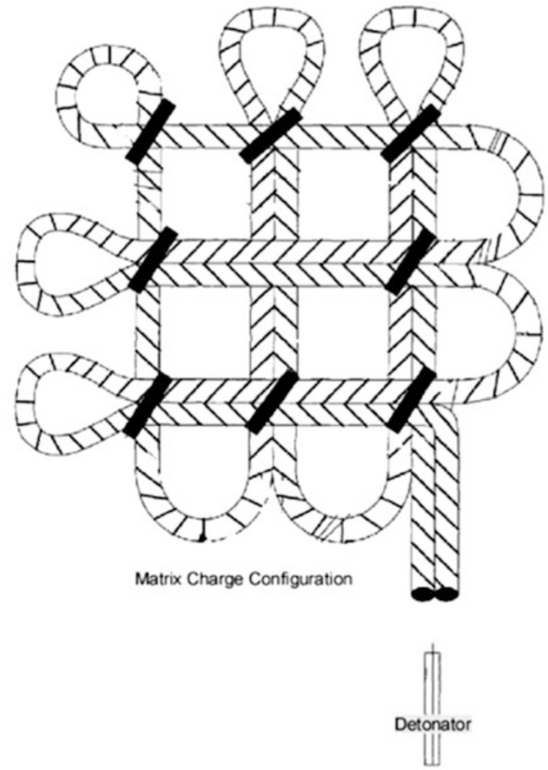

Fig. 44.1 Matrix charge; detonating cord "Net"

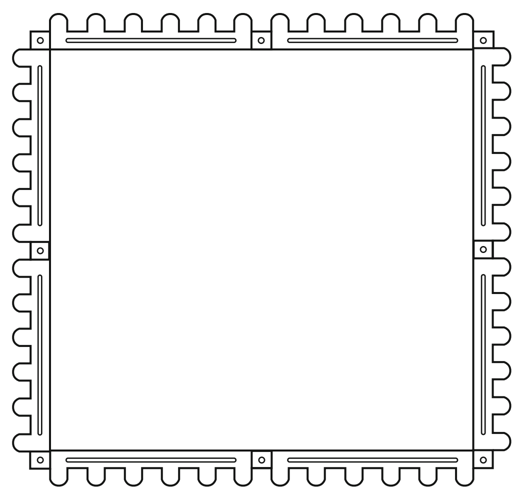

Fig. 44.2 Matrix field assembly tool

All test charges were initiated using a Reynolds Industries Systems Incorporated EBW Firing System (Fig. 44.5). The firing system triggers, lighting and SIMX camera synchronization was achieved through the use of a Stanford Research Systems, Model DG535, Four Channel Digital Delay/Pulse Generator (Fig. 44.6). The test charges were prepared and placed underwater in an aquarium within the small-scale blast chamber. The test charges were suspended from an aluminum frame for ease of handling and precise placement within the aquarium (Fig. 44.7).

The test changes consisted of sheet explosives and various geometries of detonating cord changes, see Table 44.1 for a list of the charges. Figure 44.7 shows an example of the detonating cord square configuration.

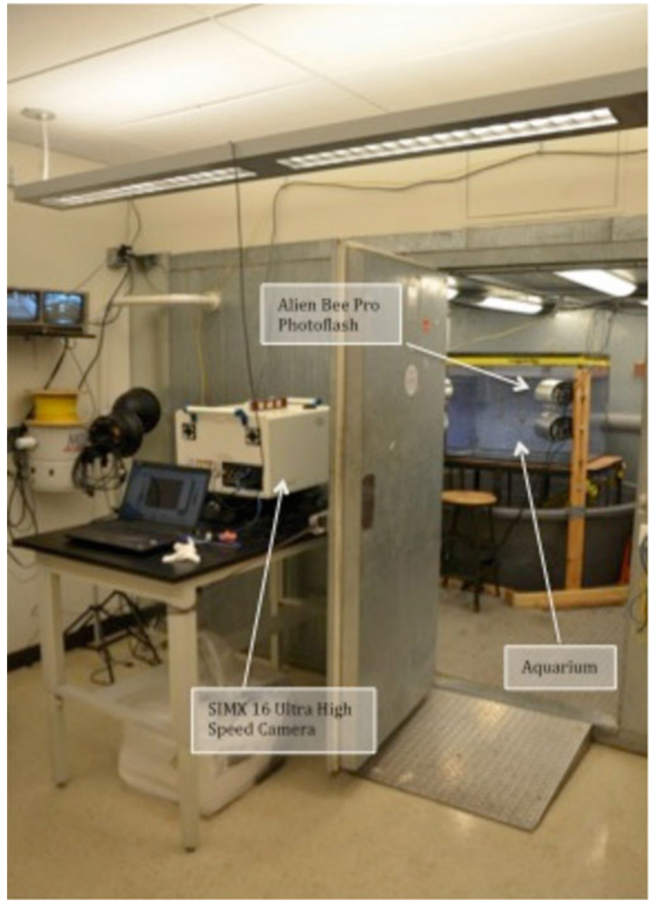

Fig. 44.3 Photo of small scale explosives laboratory showing testing set-up

44.3 Results and Analysis

The test results enabled the team to observe and measure VOD and shock wave behavior in each test charge. The team successfully recorded and documented sixteen (16) detonation events using ultra high-speed imaging technology. The ultra high-speed imagery permitted the team to visualize and measure VOD values in each test charge. The team measured and calculated VOD values consistent with detonating cord and sheet explosives VOD values reported by the manufacturer [1] and other sources [2].

Sheet explosive tests consisted of 7.62 × 7.62 cm, or 3 in., square charges (58.06 cm^2 total charge area). Figure 44.8 shows the detonation front propagating symmetrically outward from the center of the charge (point of initiation). Results show the average VOD of the sheet explosives charge is 6,984.7 ms^{-1}.

The charges produced a single, symmetrical and uniform incident shock wave at an average velocity of 1,665.3 ms^{-1}, which decayed an average of 16.5 % over a distance of 12.65 cm (acoustic velocity in water at room temperature is 1,484.7 ms^{-1}) as seen in Fig. 44.8. Side view experiments as shown in Fig. 44.9, confirmed that detonation from the center of the sheet explosive charge produced an elliptical incident shock wave, which over time transitioned to a spherical shock wave in the water.

The Matrix charge tests consisted of three different charge geometries, a single segment, a cross configuration, and a square configuration. These configurations are detailed in Table 44.1 of the previous section. These geometries were selected as a way to break down the Matrix charge into its basic components. This enabled the analysis to begin with the simplest component of the Matrix charge, a single segment of detonating cord. Figure 44.10 shows the detonation front position in two different high-speed images. This was used to calculate the average VOD, of 6,842.7 ms^{-1} for the detonating cord.

The figure also shows the formation of a linear uniform incident shock wave. This is similar to results reported by Cole in 1965 [3]. The shock wave produced by the single segment of detonating cord is similar to the shock wave produced by the sheet explosive, in that is uniform. The shape of the shock was produced are different, but both are symmetrical. Results show the average shock wave velocity was 1,787.3 ms^{-1}.

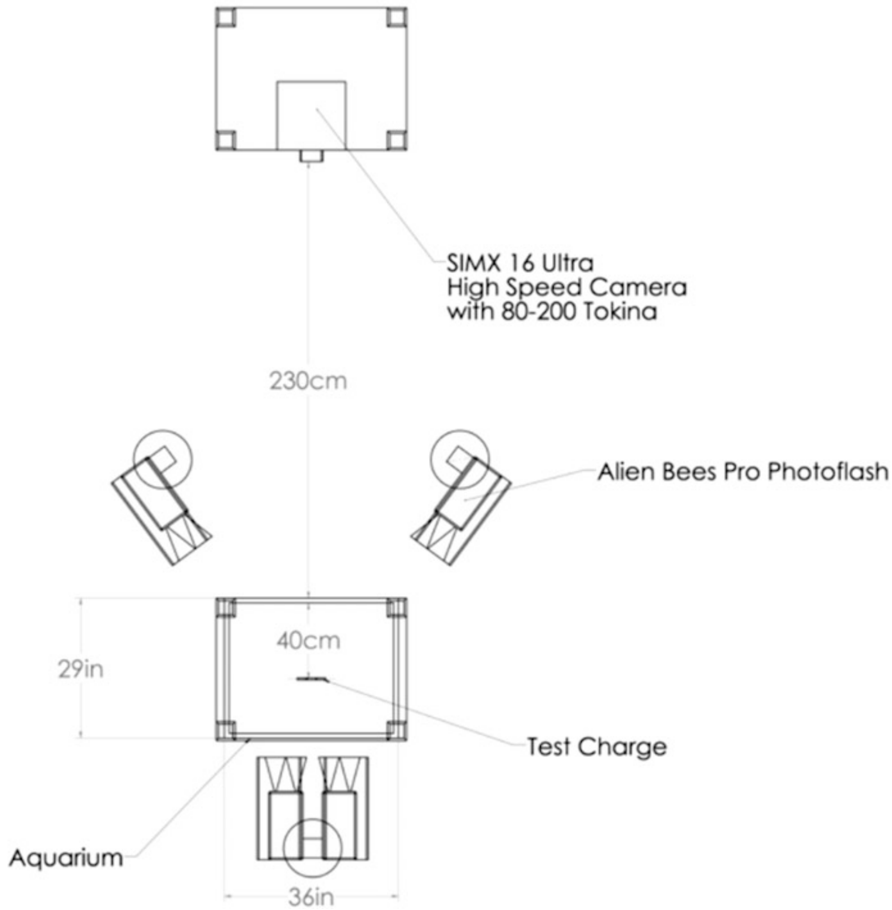

Fig. 44.4 Plan view drawing of testing set-up

Fig. 44.5 Reynolds industries systems incorporated EBW firing system

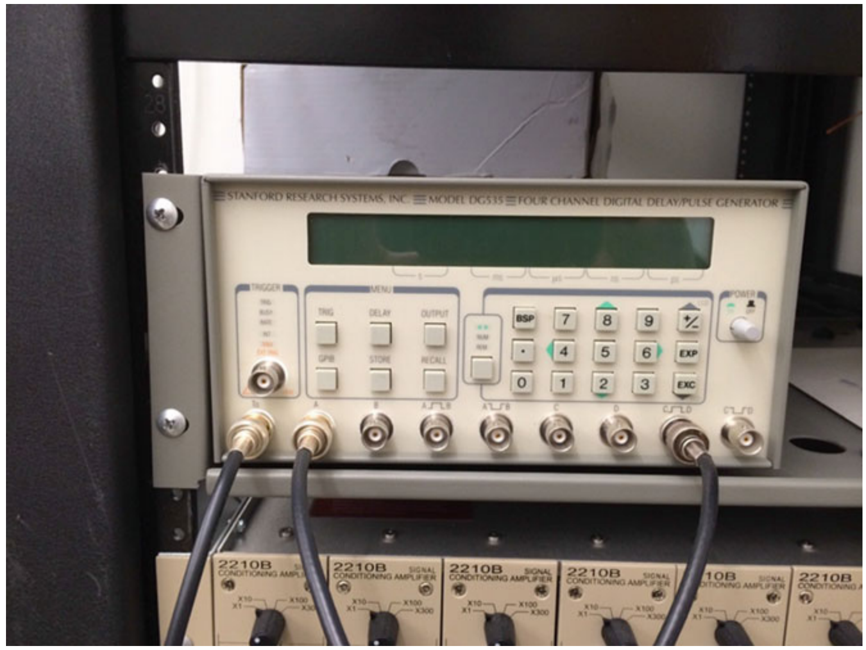

Fig. 44.6 Stanford research systems, model DG535, four channel digital delay/pulse generator

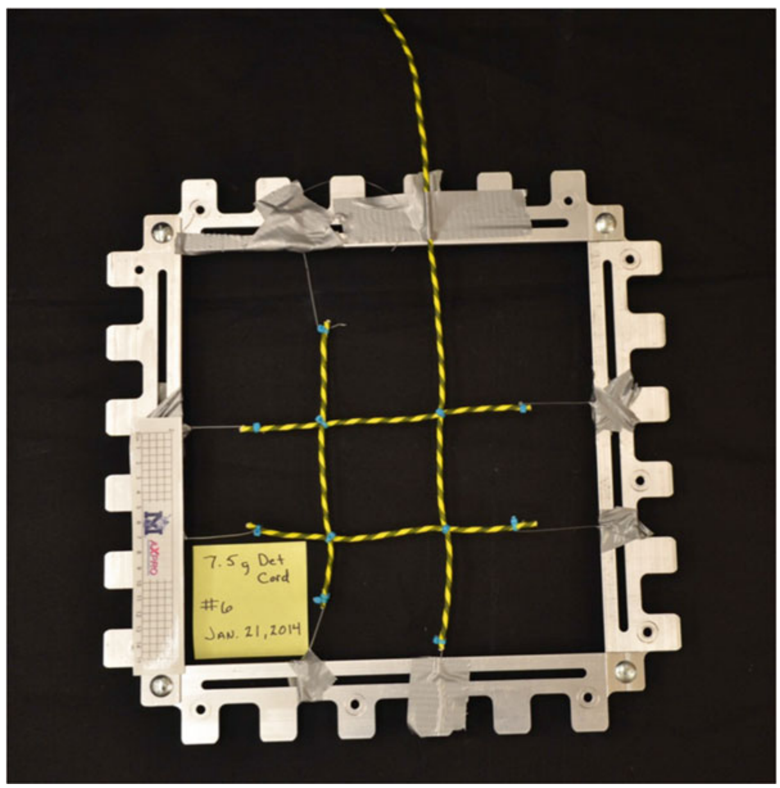

Fig. 44.7 Aluminum frame used to suspend charges in aquarium

Table 44.1 Detailed description of test charges

Test #	Initiation (priming) location All charges initiated with a RISI model RP80 EBW detonator	Charge description	Charge geometry All charges made with 7.5 grain detonating cord	Charge orientation to instrumentation	Distance of charge to front/back of aquarium (cm)
01	Secured to the upper most segment of charge	Detonating cord single segment	40 cm length suspended vertically	Frontal	42/35
02	Secured to the upper most segment of charge	Detonating cord single segment	20 cm length suspended vertically	Frontal	36/42
03	Secured to the upper most segment of charge	Detonating cord single segment	20 cm length suspended vertically	Frontal	37/40
04	Secured to the upper most segment of vertically suspended cord 30 cm from intersection of horizontally suspended cord	Detonating cord cross	68 cm length suspended vertically and intersecting a 22 cm length of horizontally suspended	Frontal	39/40
05	Secured to the upper most segment of vertically suspended cord 20 cm from intersection of horizontally suspended cord	Detonating cord cross	50 cm length suspended vertically and intersecting a 25 cm length of horizontally suspended	Frontal	36/40
06	Secured to the upper most segment of vertically suspended cord 29 cm from intersection of horizontally suspended cord	Detonating cord cross	50 cm length suspended vertically and intersecting a 15 cm length of horizontally suspended	Frontal	36/39
07	Secured to the upper most segment of vertically suspended cord 30 cm from intersection of horizontally suspended cord	Detonating cord cross	70 cm length suspended vertically and intersecting a 25 cm length of horizontally suspended	Frontal	37/39
08	Secured to the upper most segment of vertically suspended cord 30 cm from intersection of horizontally suspended cord	Detonating cord cross	70 cm length suspended vertically and intersecting a 15 cm length of horizontally suspended	Frontal	37/39
09	Secured to the upper most segment of vertically suspended cord 23 cm from intersection of horizontally suspended cord	Detonating cord cross	70 cm length suspended vertically and intersecting a 15 cm length of horizontally suspended	Side axis	18/18
10	Secured to the upper most segment of vertically suspended cord 26 cm from intersection of horizontally suspended cord	Detonating cord square	70 cm length suspended vertically, intersecting, at 26 cm, horizontally suspended 20 cm length; intersecting a second horizontally suspended 20 cm length segment, at 41 cm. Each horizontally suspended segment also intersected a second vertically suspended 30 cm segment of detonating cord 7.62 cm from original intersections. This configuration forms a 7.62 $\times$ 7.62 cm rectangular charge	Frontal	40/38

11	Secured to the upper most segment of vertically suspended cord 21 cm from intersection of horizontally suspended cord	Detonating cord square	70 cm length suspended vertically, intersecting horizontally suspended 20 cm length, at 21 cm and intersecting a second horizontally suspended segment at 36 cm. Each horizontally suspended segment also intersected a second vertically suspended 30 cm segment, 7.62 cm from original intersections. This configuration forms a 7.62 × 7.62 cm rectangular charge	Frontal	40/38
12	Secured to the upper most segment of vertically suspended cord 29 cm from intersection of horizontally suspended cord	Detonating cord square	70 cm length suspended vertically, intersecting horizontally suspended 20 cm length at 29 cm and intersecting a second horizontally suspended segment of at 44 cm. Each horizontally suspended segment also intersected a second vertically suspended 30 cm segment of detonating cord 7.62 cm from original intersections. This configuration forms a 7.62 × 7.62 cm rectangular charge	Frontal	40/38
13	Secured to the upper most segment of vertically suspended cord 27 cm from intersection of horizontally suspended cord	Detonating cord square	70 cm length suspended vertically, intersecting horizontally suspended 20 cm length at 271 cm and intersecting a second horizontally suspended segment at 42 cm. Each horizontally suspended segment also intersected a second vertically suspended 30 cm segment 7.62 cm from original intersections. This configuration forms a 7.62 × 7.62 cm rectangular charge	Side axis	18/18
14	Secured to the upper most corner segment of the charge	Sheet explosive	7.62 × 7.62 cm segment of sheet explosives (deta-sheet) vertically suspended.	Frontal	39/40
15	Secured to the center of the charge	Sheet explosives	7.62 × 7.62 cm segment of sheet explosives (deta-sheet) vertically suspended	Frontal	36/41
16	Secured to center of the charge	Sheet explosives	7.62 × 7.62 cm segment of sheet explosives (deta-sheet) horizontally suspended	Side axis	37/33

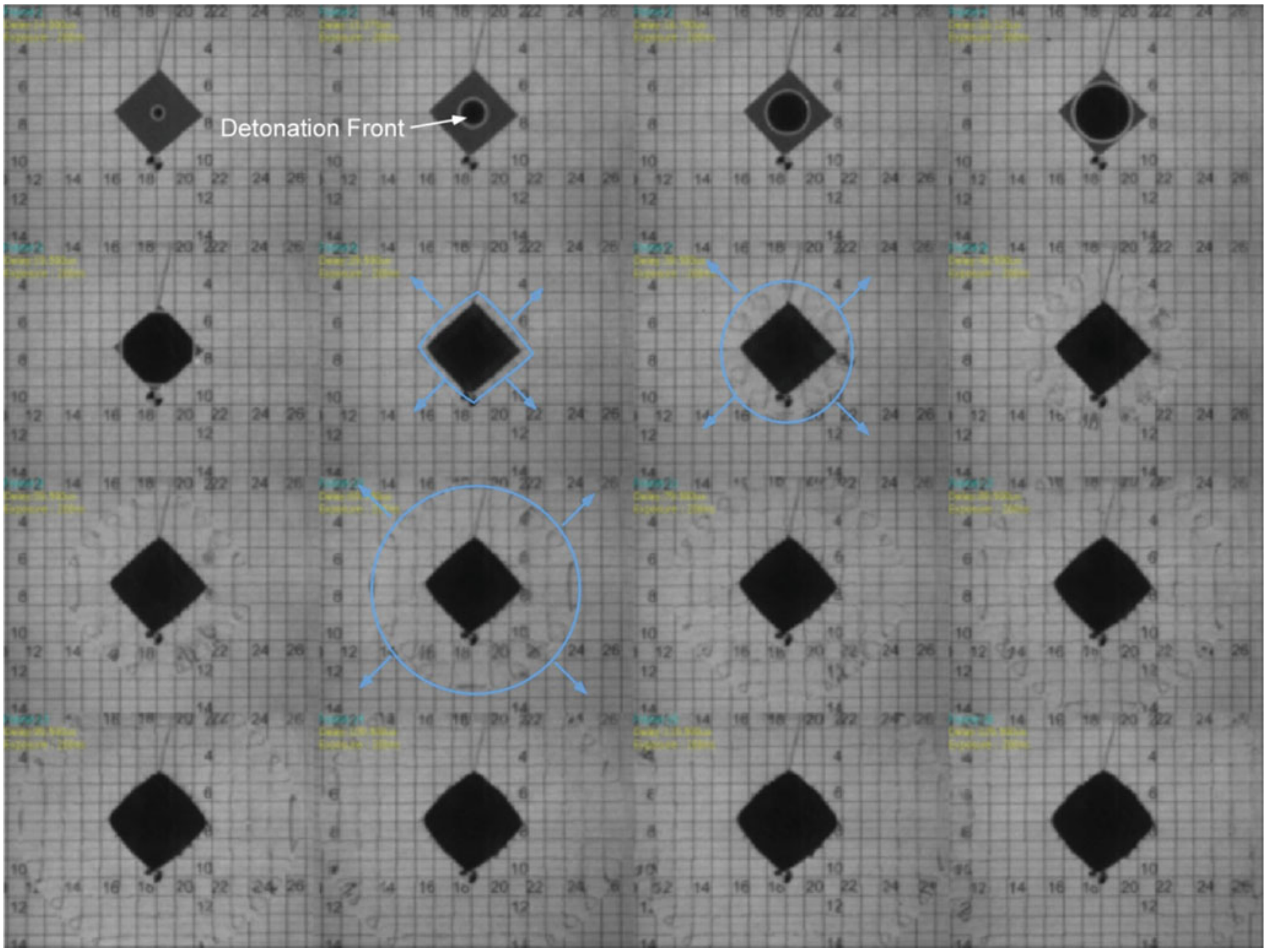

Fig. 44.8 Ultra high speed images of sheet explosive, test # 15

The next geometry tested was a cross configuration of detonating cord (Fig. 44.11). The perpendicular intersection of two segments of detonating cord allows the detonation front to propagate equally from the intersection point through each segment of detonating cord. The intersection point of detonating cord produces two additional concurrent detonation fronts. These detonation fronts form incident shock waves, which later converge and begin to produce the first visual evidence of complex shock wave interaction.

The detonating cord square configuration is consistent with the Matrix charge geometry, which consists of a series of vertically and horizontally intersecting detonating cord, the “net” shown in Fig. 44.1. The tests confirm that the detonation front propagates from each intersection along each perpendicular segment of detonating cord. The geometry and design (pattern) of the Matrix detonating cord charge enable the detonation front to propagate through the charge along right angles at precise intervals. This is shown in Figs. 44.12 and 44.13.

The additional complexity of four intersections in the square configuration produces nine total incident shock waves that then interact, converge, collide and reflect (Fig. 44.14). The turbulent nature of these shock wave interactions generates Mach stem waves [4–6], which enhances energy and pressure (Fig. 44.15).

Results validate the Matrix charge propagates predictably at right angles along each “grid” intersection and produces complex and chaotic shock waves, not seen with sheet explosive charges or other similar charges that produce detonation fronts along a linear plane.

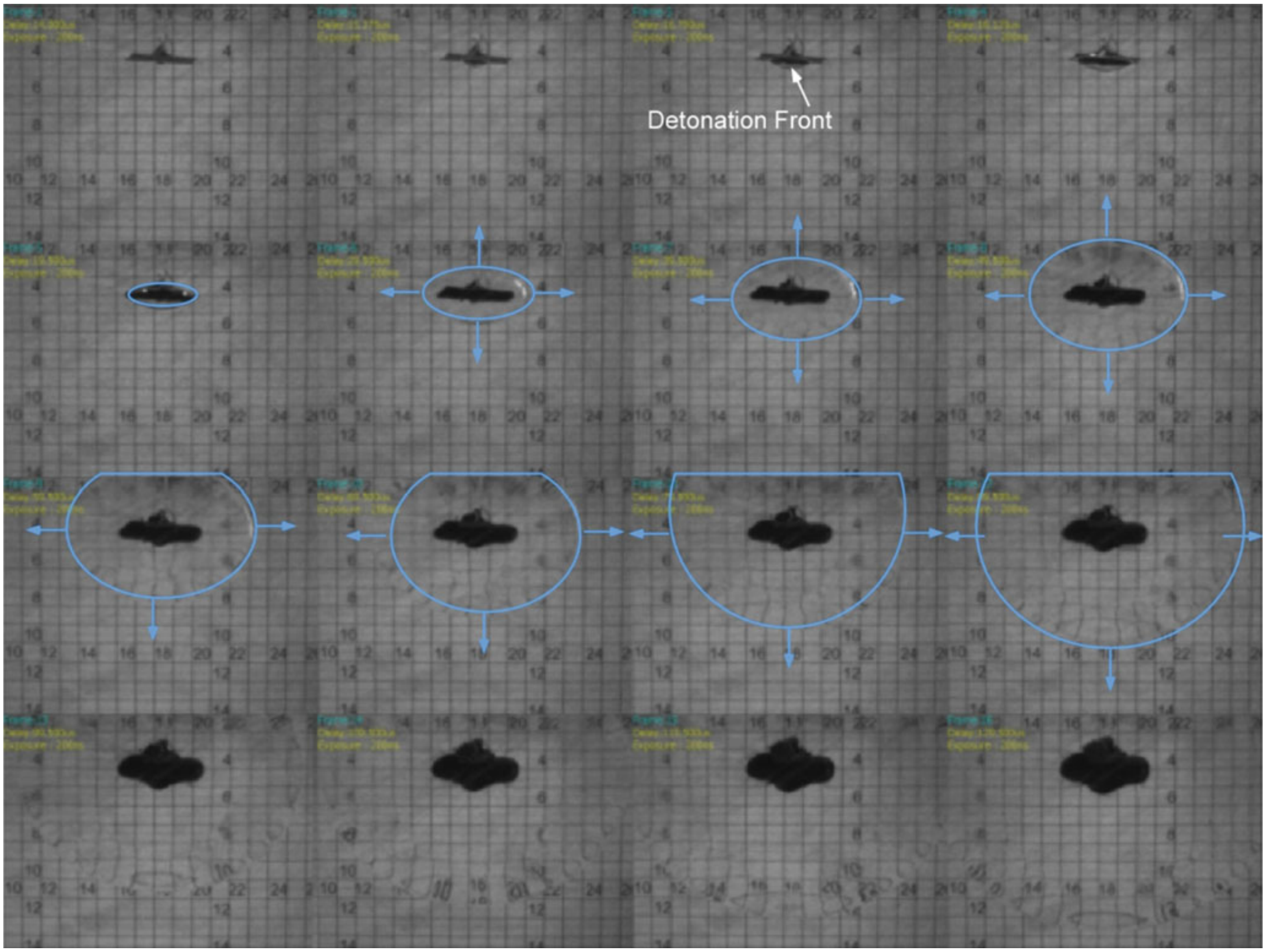

Fig. 44.9 Ultra high-speed images of sheet explosive, side view, test # 16

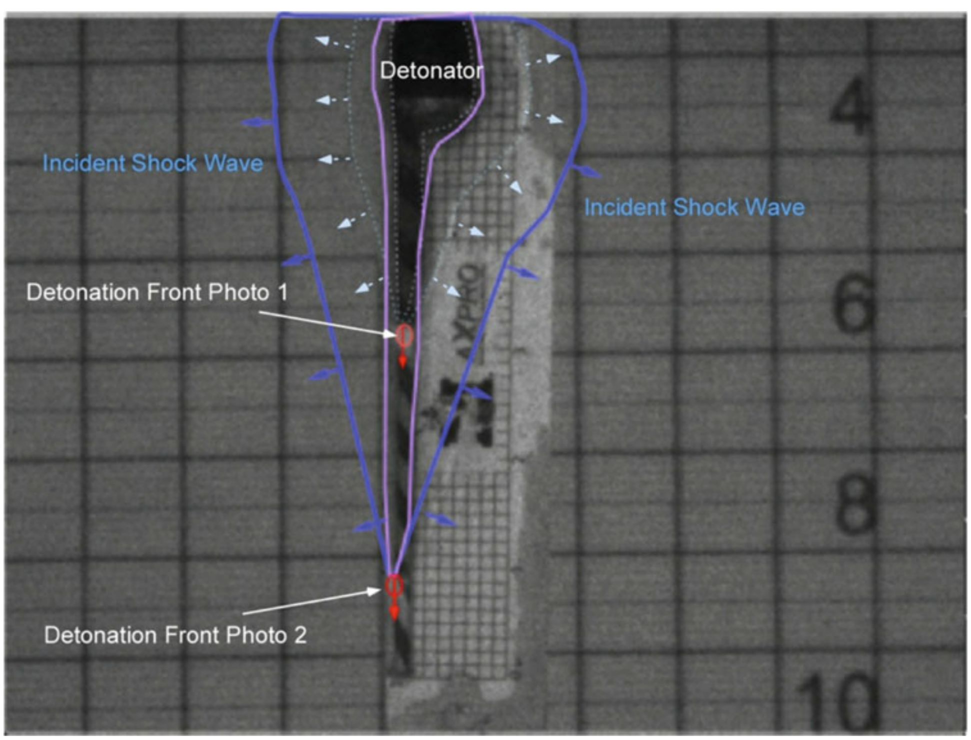

Fig. 44.10 Single segment of detonating cord

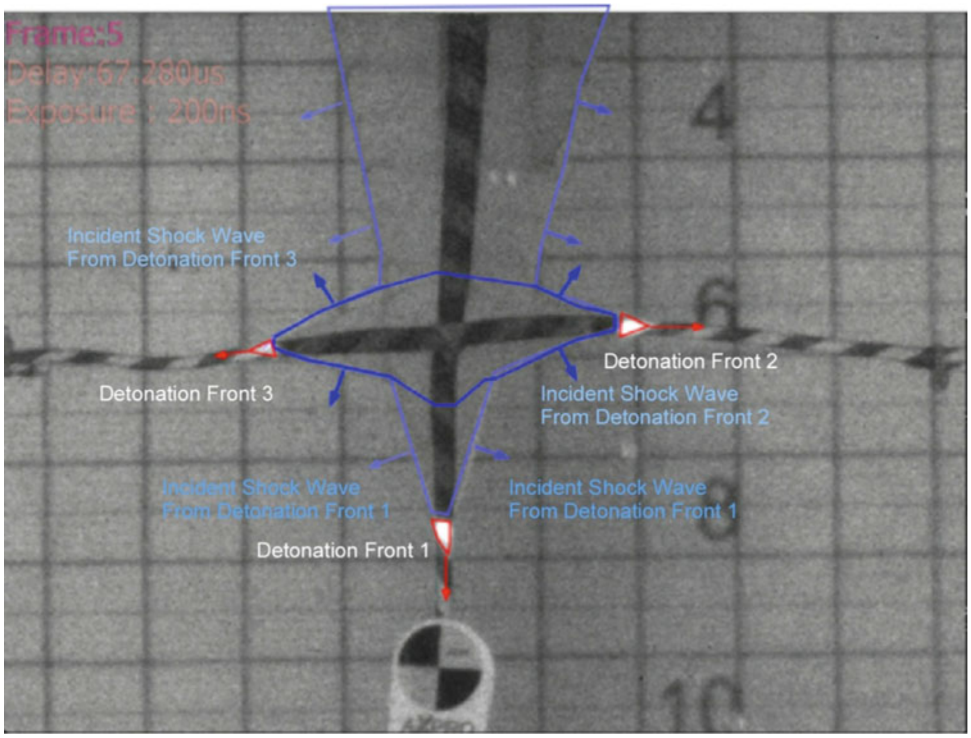

Fig. 44.11 Cross configuration of detonating cord

Fig. 44.12 Square configuration of detonating cord

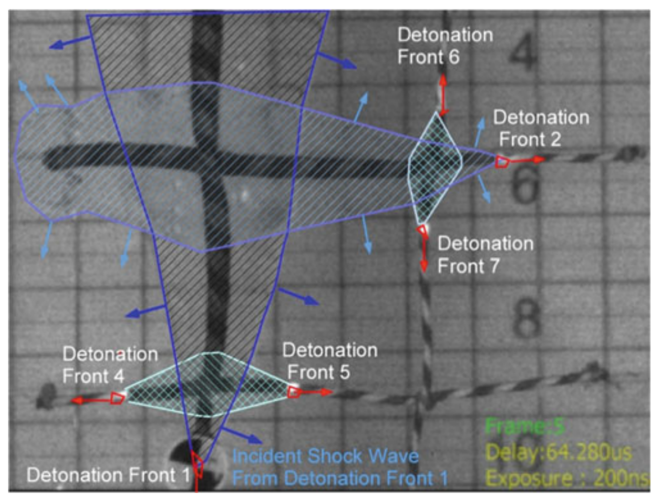

Fig. 44.13 Side view of square configuration

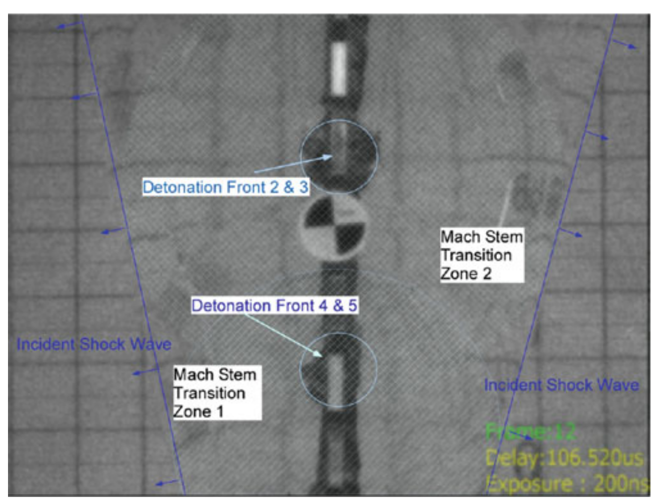

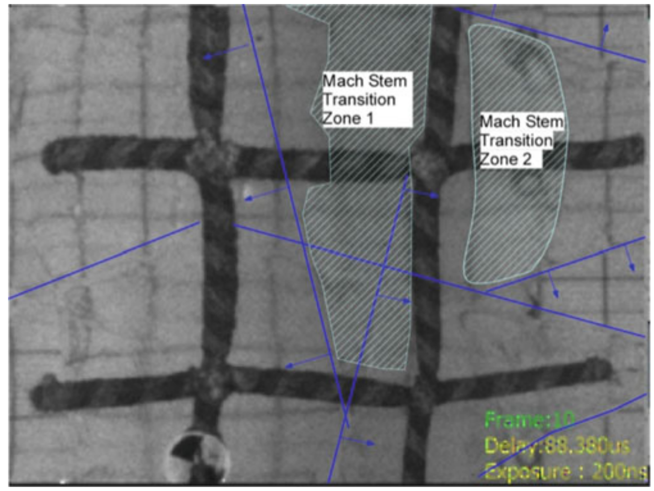

Fig. 44.14 Complex shock wave interaction

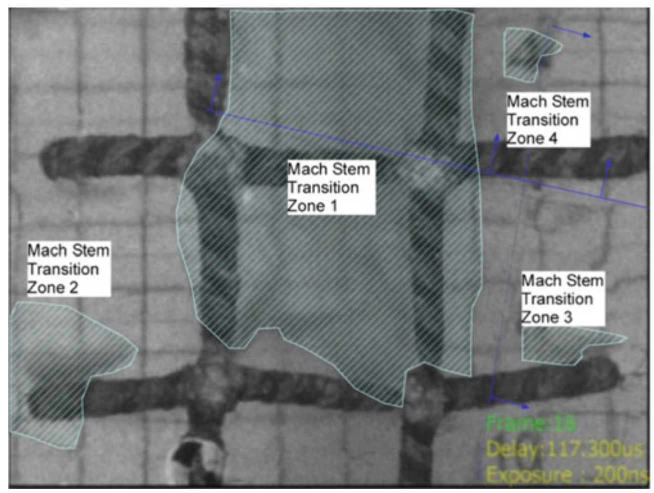

Fig. 44.15 Mach stem

44.4 Conclusions

The test results advance the understanding of the propagation and functionality of the Matrix charge configuration. Test results provided sufficient data to precisely measure VOD in all test charges and to contrast and compare the functionality of the Matrix charge configuration to sheet explosives. The tests successfully documented numerous detonation events, which enable partial characterization of the Matrix charge.

The test results permit visualization of the Matrix detonation incident and validate two fundamental assumptions:

- The matrix charge propagates along right angles at each intersection and produces multiple detonation fronts
- The Matrix charge geometry produces multiple incident shock waves which interact, converge, collide and reflect to create Mach stem waves

The Matrix charge produces multiple shock wave interactions, not seen in the sheet explosives charge, which creates multiple pressure zones using Mach disc to increase pressure and temperature within the zones. The team theorizes the shock wave interaction generated by the Matrix charge produces Mach stem as the opposing shock waves interact, conflict and reflect. This turbulence produces significant energy and pressure peculiar to the Matrix geometry. However, additional experimental testing is needed to further characterize reflected shock wave velocity and pressure. The tests provide evidence to support the use of the Matrix charge configuration in applications such as industrial cleaning, bomb disablement and avalanche mitigation.

Acknowledgments The project team wishes to express appreciation to ATF NCETR Special Agent/Program Manager Jon Mitchell, the Matrix Charge inventor of record, thus making this report possible.
All ultra high-speed images were taken by Susan Rainey, AXPRO Group Research Engineer.

References

1. Ensign-Bickford Aerospace and Defense (2012) Manufacturer of PRIMACORD, Product Technical Data Sheet
2. Netherwood Jr. PH (1985) Detonation velocity measurements of the explosives detasheet C and amatol. Memorandum Report BRL-MR-3427, Jan 1985
3. Cole RH (1965) Underwater explosions. Dover Publications, New York, pp 255–258
4. Ben-Dor G (2007) Shock wave reflection phenomena, 2nd edn. Springer, Berlin, pp 144–146, 293
5. Krehl P, Van Der Gest M (1991) The discovery of the Mach reflection effect and its demonstration in an auditorium. J Shock Wave 1:3–15, Springer
6. Cornish V (1910) Wave of the sea and other water waves. T Fisher Unwin, London, p 173